Electrocatalytic Voltammetry of Succinate Dehydrogenase: Direct Quantification of the Catalytic Properties of a Complex Electron-Transport Enzyme

Judy Hirst,[†] Artur Sucheta,[‡] Brian A. C. Ackrell,[§] and Fraser A. Armstrong*,[†]

Contribution from the Inorganic Chemistry Laboratory, South Parks Road, Oxford OX1 3QR, England, and VA Hospital and Department of Biochemistry and Biophysics, Molecular Biology Division, University of California, San Francisco, California 94121

Received October 11, 1995[⊗]

Abstract: Succinate dehydrogenase (SDH), the membrane-extrinsic component of Complex II, adsorbs at a pyrolytic graphite edge electrode and catalyzes interconversion of succinate and fumarate depending on the electrochemical potential that is applied. The catalytic activity is measured over a continuous potential range, leading to a quantitative description of the interlinked energetics and kinetics of catalyzed electron transport, including the degree to which the enzyme is intrinsically tuned, at a particular pH, to function either in the direction of succinate oxidation or fumarate reduction. It is revealed that under reversible conditions (i.e. near the reduction potential of the fumarate/succinate couple) and at the physiological temperature of 38 °C, SDH is biased to catalyze fumarate reduction (reversal of the tricarboxylic acid cycle) at pH values below 7.7. Subtle effects which gate electron transport are detected. First, the sharp drop in catalytic activity observed as the potential is made more negative is an intrinsic property that is associated with two-electron/two-proton reduction of the FAD, and second, binding and release of the competitive inhibitor/regulator oxalacetate is observed as the enzyme is cycled between FAD_{ox} (tight binding) and FAD_{red} (weaker binding) states. It is thereby demonstrated how the electron-transport characteristics of a complex redox enzyme, integrating both kinetic and thermodynamic information, can be derived from voltammetric experiments.

1. Introduction

The question of how multi-centered redox metalloenzymes catalyze electron transport and coupled reactions is of great importance for the understanding of biological energy transduction. The structural basis for some of these processes is revealed in several recent crystal structures, including ascorbate oxidase, nitrogenase, hydrogenase, and cytochrome *c* oxidase.[1] Typically, the sites for catalytic transformations are "wired" by one or more redox centers which mediate electron transfer into or across the enzyme[2] and may also be involved in regulation or coupling to reactions such as ion binding or pumping. However, the various kinetic and spectroscopic techniques traditionally used to study electron-transport tend to produce a collage of separate informational items rather than immediate visualization of a more unified picture. In recent years it has become feasible to perform direct, dynamic electrochemical measurements on redox proteins[3,4] with the most refined information stemming from studies in which the protein is adsorbed as an electroactive film.[5−15] For enzymes, the ability to obtain a "direct read-out" of the catalytic action once "plugged into" an electrochemical analyzer offers attractive prospects for

* Address correspondence to this author.
† Inorganic Chemistry Laboratory.
‡ Current address: Department of Chemistry, University of California Santa Cruz, Santa Cruz, CA 95064.
§ University of California.
⊗ Abstract published in *Advance ACS Abstracts,* April 15, 1996.

(1) Messerschmidt, A.; Lücke, H.; Hüber, R. *J. Mol. Biol.* **1993**, *230*, 997−1014 and references therein. Kim, J. S.; Rees, D. C. *Nature* **1992**, *360*, 553−560. Georgaiadis, M. M.; Komiya, H.; Chakrabarti, P.; Woo, D.; Kornuc, J. J.; Rees, D. C. *Science* **1992**, *257*, 1653−1659. Volbeda, A.; Charon, M-H.; Piras, C.; Hatchikian, E. C.; Frey, M.; Fontecilla-Camps, J. C. *Nature* **1995**, *373*, 580−587. Iwata, I.; Ostermeier, C.; Ludwig, B.; Michel, H. *Nature* **1995**, *376*, 660−669. Tsukihara, T.; Aoyama, H.; Yamashita, E.; Tomikazi, T.; Yamaguchi, H.; Shinzawa-Itoh, K.; Nakashima, R.; Yaono, R.; Yoshikawa, S. *Science* **1995**, *269*, 1069−1074.

(2) Moser, C. C.; Keske, J. M.; Warncke, K.; Farid, R. S.; Dutton, P. L. *Nature* **1992**, *355*, 796−802. Beratan, D. N.; Betts, J. N.; Onuchic, J. N. *Science* **1991**, *252*, 1285−1288.

(3) Armstrong, F. A. In *Advances in Inorganic Chemistry*; Cammack, R., Sykes, A. G., Eds.; Academic Press: San Diego, 1993; Vol. 38, pp 117−163. Armstrong, F. A. *Structure Bonding* **1990**, *72*, 137−230. Bond, A. M.; Hill, H. A. O. In *Metal Ions in Biological Systems*; Sigel, H., Sigel, A., Eds.; Marcel Dekker: New York, 1991; Vol. 27, Chapter 12, pp 431−494. Armstrong, F. A.; Butt, J. N.; Sucheta, A. *Methods Enzymol.* **1993**, *223*, 479−500.

(4) Büchi, F. N.; Bond A. M. *J. Electroanal. Chem.* **1991**, *314*, 191−206. Bond A. M. *Anal. Proc.* **1992**, *29*, 132−148.

(5) Willit, J. L.; Bowden, E. F. *J. Phys. Chem.* **1990**, *94*, 8241−8246. Bowden, E. F.; Clark, R. A.; Willit, J. L.; Song, S. In *Redox Mechanisms and Interfacial Properties of Molecules of Biological Importance*; Schultz, F. A., Taniguchi, I., Eds.; The Electrochemical Society Inc., 1993; pp 34−45.

(6) Hildebrandt, P. *J. Mol. Struct.* **1991**, *242*, 379−395. Collinson, M.; Bowden, E. F. *Anal. Chem.* **1992**, *64*, 1470−1476.

(7) Butt, J. N.; Armstrong, F. A.; Breton, J.; George, S. J.; Thomson, A. J.; Hatchikian, E. C. *J. Am. Chem. Soc.* **1991**, *113*, 6663−6670. Butt, J. N.; Sucheta, A.; Armstrong, F. A.; Breton, J.; Thomson, A. J.; Hatchikian, E. C. *J. Am. Chem. Soc.* **1991**, *113*, 8948−8950. Butt, J. N.; Sucheta, A.; Armstrong, F. A.; Breton, J.; Thomson, A. J.; Hatchikian, E. C. *J. Am. Chem. Soc.* **1993**, *115*, 1413−1421. Butt, J. N.; Niles, J.; Armstrong, F. A.; Breton, J.; Thomson, A. J. *Nature Struct. Biol.* **1994**, *1*, 427−433. Shen, B.; Martin, L. L.; Butt, J. N.; Armstrong, F. A.; Stout, C. D.; Jensen, G. M.; Stephens, P. J.; La Mar, G. N.; Gorst, G. M.; Burgess, B. K. *J. Biol. Chem.* **1993**, *268*, 25928−25939. Butt, J. N.; Sucheta, A.; Martin, L. L.; Shen, B.; Burgess, B. K.; Armstrong, F. A. *J. Am. Chem. Soc.* **1993**, *115*, 12587−12588.

(8) Armstrong, F. A.; Lannon, A. M. *J. Am. Chem. Soc.* **1987**, *109*, 7211−7212. Scott, D. L.; Paddock, R. M.; Bowden, E. F. *J. Electroanal. Chem.* **1992**, *341*, 307−321. Scott, D. L.; Bowden, E. F. *Anal. Chem.* **1994**, *66*, 1217−1223.

(9) Bianco, P.; Haladjian, J. *J. Electrochem. Soc.* **1992**, *139*, 2428−2432.

(10) Armstrong, F. A.; Bond, A. M.; Büchi, F. N.; Hamnett, A.; Hill, H. A. O.; Lannon, A. M.; Lettington, O. C.; Zoski, C. G. *Analyst* **1993**, *118*, 973−978.

(11) Ikeda, T.; Miyaoka, S.; Miki, K. *J. Electroanal. Chem.* **1993**, *352*, 267−278.

(12) Sucheta, A.; Ackrell, B. A. C.; Cochran, B.; Armstrong, F. A. *Nature* **1992**, *356*, 361−362.

(13) Ackrell, B. A. C.; Armstrong, F. A.; Cochran, B.; Sucheta, A.; Yu, T. *FEBS Lett.* **1993**, *326*, 92−94.

S0002-7863(95)03436-6 CCC: $12.00

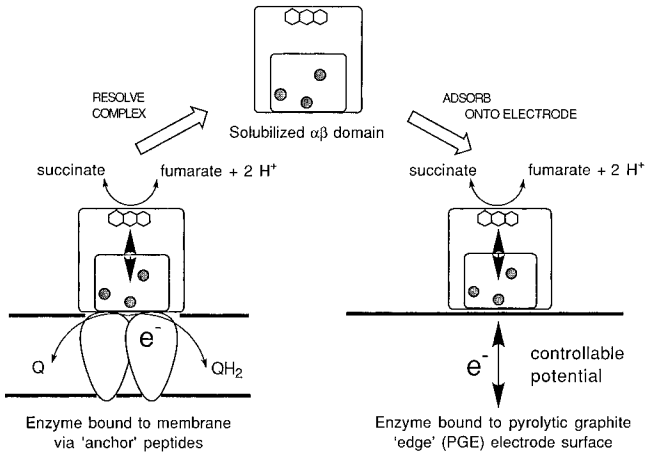

Figure 1. Schematic diagram showing the resolution of SDH (the two catalytic and membrane-extrinsic subunits) from Complex II (A) and the adsorption of SDH onto the electrode surface (B).

obtaining novel and alternative perspectives on electron-transport characteristics, analogous to determining the $i-E$ profiles of complex electronic circuit components.

Complex II (succinate−ubiquinone oxidoreductase; EC1.3.99.1) is one of the membrane-bound enzymes of the respiratory chain in aerobically respiring organisms.[16] It plays a central role in energy production by providing a direct link between the tricarboxylic acid (TCA) cycle and the membrane-bound electron-transport (oxidative phosphorylation) system. Electrons are exchanged between aqueous fumarate/succinate and the lipid-localized (ubi)quinone pool, according to eqs 1A and 1B.

$$\text{fumarate} + 2e^- + 2H^+ \rightleftharpoons \text{succinate} \qquad (1A)$$

$$Q + 2e^- + 2H^+ \rightleftharpoons QH_2 \qquad (1B)$$

As illustrated by the cartoon in Figure 1, Complex II is composed of four non-identical subunits organized into two domains. The membrane-extrinsic "catalytic" domain comprises two hydrophilic subunits, F_p and I_p, having approximate molecular masses of 70 000 and 27 000, respectively, while the membrane-intrinsic domain consists of two hydrophobic "anchor" peptides which allow interaction with the quinone pool.[16] Subunit F_p contains a covalently bound FAD (flavin adenine dinucleotide) and the site of substrate binding, whereas I_p contains three iron−sulfur clusters—[2Fe−2S], [4Fe−4S], and [3Fe−4S]—Centers 1, 2, and 3, respectively. A *b*-type cytochrome is associated with the hydrophobic domain. The FAD exhibits a cooperative two-electron reduction reaction, with the semiquinone radical attaining only a low concentration.[17] Reduction potentials for successive one-electron reductions of the FAD at pH 7.0 are reported to be $E_1 = -128$ mV and $E_2 = -30$ mV respectively, thus $E_{12} = -79$ mV.[17,18] Reported potentiometric values for the Fe−S clusters are as follows: Center 1, 0 mV; Center 2, −260 mV; Center 3, 60 mV.[16,19] Values determined for the substrate couples fumarate/succinate (0 ± 10 mV vs SHE at 30 °C)[20] and ubiquinone/ubiquinol (within a broad range, E_1 ($Q/Q^{\bullet-}$) = +40 to +110 mV, E_2 ($Q^{\bullet-}/QH_2$) = +50 to +80 mV)[21] indicate the thermodynamic reversibility of the catalyzed reaction, which is not capable of powering proton translocation. Complex II can be resolved to give a water-soluble enzyme, consisting only of the catalytic domain, which retains the ability to catalyze reduction of fumarate or oxidation of succinate by artificial electron donors or acceptors, but is unable to catalyze the reaction with quinones.[16] The soluble form is referred to as succinate dehydrogenase (SDH).

Recently it has been shown that SDH adsorbs at a pyrolytic graphite "edge" (PGE) electrode to form an electrocatalytically active film, apparently of low surface coverage.[12] As a working hypothesis, this process (Figure 1) creates a situation in which the enzyme accepts the electrode as a binding site and redox partner in place of the anchor peptides and membrane-bound quinone pool. The high level of reversible electrocatalytic activity that is displayed permits the catalytic performance (current is a direct measurement of overall rate) to be probed in detail by scanning over a continuously variable range of potential. Catalysis of succinate oxidation in the reversible region was observed to proceed in the manner expected for a reaction that is controlled by the thermodynamic driving force, i.e. the rate increases rapidly as the potential is increased. By contrast, catalyzed fumarate reduction appears to be under thermodynamic control at potentials in the region of the fumarate/succinate couple, but shows a sharp drop in activity once a critical value of the potential is exceeded.[12,22] We referred to this as the "tunnel diode" effect because of the similarity with the electronic device that exhibits negative resistance over a certain range of potential bias.[12,23] For SDH from several sources, the predicted inverse relationship between driving force and rate of fumarate reduction was found to be exhibited in non-electrochemical steady-state kinetic experiments in which benzyl viologen was used as electron donor.[13] No such effects were observed in analogous experiments with the closely related enzyme fumarate reductase.[13−15] The observation was shown to be independent of the particular nature of the electrode/enzyme interface since voltammograms recorded at gold electrodes, although giving a weak response, gave the same peak potentials, over all pH values, as those recorded at PGE electrodes.[13] The tunnel diode effect thus appeared to be an intrinsic property of SDH.

We have now studied the electrocatalytic properties of SDH in much greater detail to produce a robust database having excellent reproducibility and precision, and a straightforward theoretical model has been set up and applied. Despite the simplicity of the model, the results are accounted for extremely well at an empirical level, and subtle features of the enzyme's catalytic properties are revealed.

(14) Armstrong, F. A.; Sucheta, A.; Ackrell, B. A. C.; Weiner, J. H. In *Redox Mechanisms and Interfacial Properties of Molecules of Biological Importance*; Schultz, F. A., Taniguchi, I., Eds.; The Electrochemical Society Inc., 1993; pp 184−196.

(15) Sucheta, A.; Cammack, R.; Weiner, J.; Armstrong, F. A. *Biochemistry* **1993**, *32*, 5455−5465.

(16) Ackrell, B. A. C.; Johnson, M. K.; Gunsalus, R. P.; Cecchini, G. In *Chemistry and Biochemistry of Flavoenzymes*; Müller, F., Ed.; CRC Press: Boca Raton, FL, 1992. Hederstedt, L.; Ohnishi, T. In *Molecular Mechanisms in Bioenergetics*; Ernster, L., Ed.; Elsevier: New York, 1992; pp 163−198.

(17) Ohnishi, T.; King, T. E.; Salerno, J. C.; Blum, H.; Bowyer, J. R.; Maida, T. *J. Biol. Chem.* **1981**, *256*, 5577−5582.

(18) Ackrell, B. A. C.; Kearney, E. B.; Edmondsen, D. *J. Biol. Chem.* **1975**, *250*, 7114−7119.

(19) Ohnishi, T.; Lim, J.; Winter, D. B.; King, T. E. *J. Biol. Chem.* **1976**, *251*, 2105−2109. Ohnishi, T.; Salerno, J. C.; Winter, D. B.; Lim, J.; Yu, C.-A.; King, T. E. *J. Biol. Chem.* **1976**, *251*, 2094−2104. Maguire, J. L.; Johnson, M. K.; Morningstar, J. E.; Ackrell, B. A. C.; Kearney, E. B. *J. Biol. Chem.* **1985**, *260*, 10909−10912.

(20) Clark, W. M. In *Oxidation-Reduction Potentials of Organic Systems*; Baillière, Tindall & Cox Ltd.: London, 1960.

(21) Salerno, J. C.; Oshnishi, T. *Biochem. J.* **1980**, *192*, 769−781.

(22) A similar observation has been reported for another metalloflavoenzyme, D-gluconate dehydrogenase (ref 11).

(23) Mackenroth, D. R.; Sands, L. G. In *Illustrated Encyclopaedia of Solid-State Circuits and Applications*; Prentice Hall: Englewood Cliffs, NJ, 1984; Chapter 1.

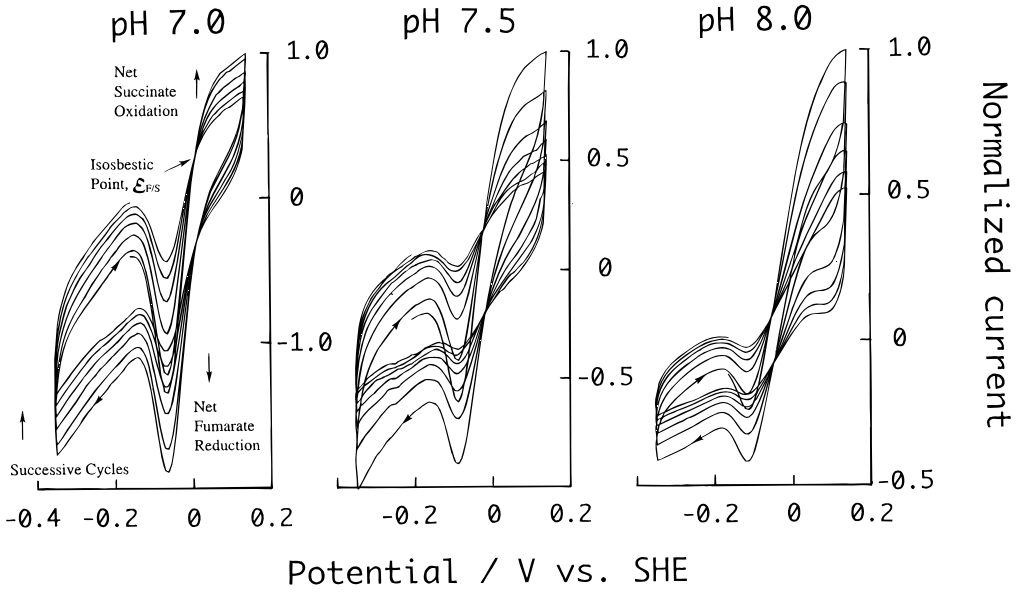

Figure 2. Cyclic voltammograms observed at an edge-orientated pyrolytic graphite electrode for 1:1 solutions of fumarate and succinate at 38 °C in the presence of succinate dehydrogenase (1 μM). Scan rate 10 mV s^{-1}, rotation rate 500 rpm. The enzyme was added to the solution immediately before inserting the electrode, which was then poised at −400 mV for 30 s prior to commencing scans. Electrolyte compositions are given in the Experimental Section. From left to right: pH 7.0, substrate concentrations 0.13 mM; pH 7.5, substrate concentrations 0.59 mM; pH 8.0, substrate concentrations 0.59 mM. For comparative purposes the currents have been normalized to a maximum oxidation current of 1; typical observed currents were around 15 μA cm^{-2}.

2. Experimental Section

Pure SDH was isolated according to the procedure described by Davis and Hatefi, in which isolated Complex II is resolved using perchlorate.[24,25] The enzyme was stored as ammonium sulfate pellets in liquid nitrogen. Enzyme concentrations were obtained using the biuret method after precipitation with trichloroacetic acid.[26] All voltammetric experiments and handling of enzyme solutions were carried out in a glovebox (Vacuum Atmospheres) under a nitrogen atmosphere (O_2 < 2 ppm). Prior to experiments, the enzyme solutions were freed of residual ammonium sulfate, perchlorate, and most of the succinate by diafiltration (Amicon 8MC, YM30 membrane) against the appropriately buffered electrolyte solutions. The supporting electrolyte consisted of 0.1 M NaCl (BDH) with a mixed buffer system composed of 10 mM HEPES (*N*-[2-hydroxyethyl]piperazine-*N*′-[2-ethanesulfonic acid]), 10 mM MES (2-[*N*-morpholino]ethanesulfonic acid), and 10 mM TAPS (*N*-tris[hydroxymethyl]methyl-3-aminopropanesulfonic acid) (all supplied by Sigma). Fumaric acid (99.5%), succinic acid (99.5%), and oxalacetic acid (99%) were purchased from Fluka. All solutions were prepared at room temperature and the pH was adjusted by addition of NaOH or HCl as necessary. Fixed ratio fumarate−succinate mixtures (typically 1:1) in experimental solutions were obtained by dilution of concentrated solutions prepared accurately by weight. Oxalacetate stock solutions were made up in MES buffer at pH 6.3 and used immediately. Following each experiment, the cell solution was retained, and its pH was measured at 38 °C.

Electrochemical experiments were carried out using an AutoLab electrochemical analyzer (Eco-Chemie, Utrecht, The Netherlands) equipped with a low-current detection module, in conjunction with a EG&G M636 electrode rotation apparatus. The all-glass, jacketed electrochemical cell and electrodes used have been described previously.[15] The apparatus was housed within a Faraday cage. Prior to each experiment the PGE electrode (area 0.03 cm^2) was polished with 1-μm alumina (Buehler) and then sonicated thoroughly. A saturated calomel electrode (SCE) was used as a reference electrode; all potentials given are adjusted to the standard hydrogen electrode (SHE) scale (E = 241 mV at 25 °C).

3. Experimental Results

General Observations. Figure 2 shows rotating disk voltammograms obtained at 10 mV s^{-1} for equimolar solutions of fumarate and succinate in the presence of 1 μM SDH, which adsorbs on the electrode.[12] Higher concentrations of enzyme did not increase the magnitude of the response. Several features are immediately apparent. First, the current due to net oxidation of succinate rises with increasing potential to reach a steady limiting value i^S_{lim}, then as the potential is taken to more negative potentials, the direction of catalysis switches over to reduction of fumarate. Second, the reduction current displays an additional potential dependence, reaching a maximum value i^F_{peak}, then falling sharply to a lower, limiting level, i^F_{lim}. The peak potential E_{peak} is the same for either scan direction.[27] Third, the activity decreases uniformly (i.e. independently of the applied potential) over the course of second and subsequent cycles,[28] generating an isosbestic point on each half of the cycle. This decrease in activity proved to be extremely useful and was exploited in our analysis. As described below, the isosbestic potential ($E_{F/S}$) is the potential at which the rate of succinate oxidation is equal to the rate of fumarate reduction, and is related in a Nernstian manner to the formal reduction potential of the fumarate/succinate couple. The isosbestic points for each direction coincide (to within 5 mV of each other) at scan rates of 10 mV s^{-1} or lower, but at higher scan rates $E_{F/S}$ (in the direction of increasing potential) ≤ $E_{F/S}$ (in the direction of decreasing potential), although the average value remains

(24) Davis, K. A.; Hatefi, Y. *Biochemistry* **1971**, *10*, 2509−2516.
(25) Beginsky, M. L.; Hatefi, Y. *J. Biol. Chem.* **1969**, *244*, 5313−5319.
(26) Gornall, A. G.; Bardawill, C. J.; David, M. M. *J. Biol. Chem.* **1949**, *177*, 756−766.
(27) There is a small but reproducible positive shift in E_{peak} values occurring with decreasing ratio of fumarate−succinate (approximately 10 mV per decade).
(28) The reasons for the decrease of the electrocatalytic response are not clear, although it is known that isolated SDH is only stable in the absence of O_2 and in the presence of high concentrations of succinate, conditions which serve to keep Center 3 reduced and intact (Beinert, H.; Ackrell, B. A. C.; Vinogradov, A. D.; Kearney, E. B.; Singer, T. P. *Arch. Biochem. Biophys.* **1977**, *182*, 95−106). Indeed, experiments conducted with high fumarate-to-succinate ratios produced extremely unstable voltammetry. However, greater stability was not obtained when cycling was restricted to potentials <60 mV, the reduction potential of Center 3.

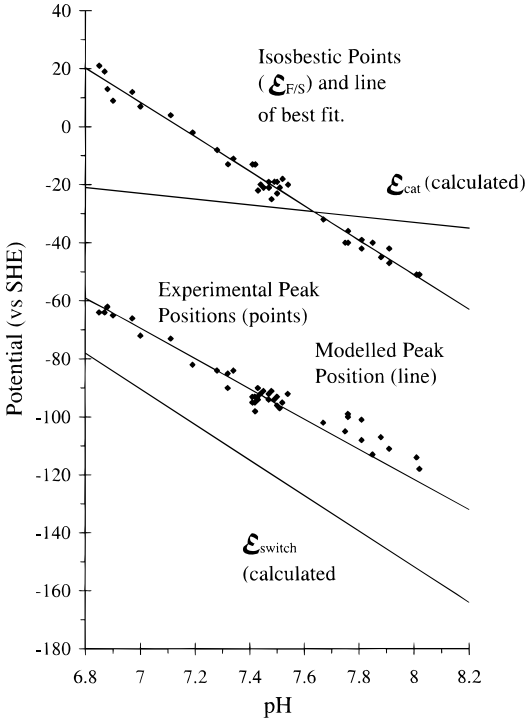

Figure 3. Experimentally determined isosbestic points and fumarate peak positions as a function of pH at 38 °C. Also shown are the modeling parameters E_{cat} and E_{Switch} and the peak positions predicted by the model.

constant. Fourth, as the pH is raised, the voltammograms change shape as the rate of succinate oxidation increases relative to the rate of fumarate reduction.

Several other features were established. It was determined that the Faradaic current response is essentially independent of the following: (i) scan rate up to at least 20 mV s^{-1} (even at a scan rate of 100 mV s^{-1} the separation of E_{peak} values is only 10 mV), (ii) electrode rotation rate at all substrate concentrations considered, and (iii) absolute substrate concentrations (for fumarate/succinate ratios of 1:1) in the range of 0.10−10 mM.[27] Consequently, the current measured at any particular potential corresponds to a condition of steady state.[29] The results were reproducible among several samples of enzyme prepared over the course of 3 years.

The Isosbestic Point. As a potential reference, the isosbestic point is equated with the electrode potential for the fumarate/succinate couple, $E_{F/S}$, operative under the experimental conditions imposed. Assuming that the enzyme acts as a true catalyst (i.e. changing only the rate of attainment of equilibrium and not its position) we expect the isosbestic point, $E_{F/S}$, to vary with fumarate, succinate, and proton activities as given by the relevant Nernst equation, eq 2.

$$E_{F/S} = E^{\circ}_{F/S} + \frac{RT}{2F}\left[\ln\left(\frac{a_{fum}}{a_{succ}}\right) - 2\cdot\ln 10\cdot pH\right] \qquad (2)$$

in which a_{fum} and a_{succ} are activities of fumarate and succinate, respectively, and $E^{\circ}_{F/S}$ is the formal reduction potential for the fumarate/succinate couple. As shown in Figure 3, the experimental data obtained with measured (1:1) concentrations of fumarate and succinate are in excellent agreement with eq 2, and the formal reduction potential applicable to pH 7.0 and 38 °C, $E^{\circ}_{F/S} \approx 10$ mV vs SHE, is very similar to published data obtained from potentiometry.[20] For data at high scan rates, where the two $E_{F/S}$ values do not coincide, the average value is reported. Further experiments conducted with varying ratios of fumarate and succinate confirmed the validity of eq 2. These results and the good agreement with potentiometric solution values show that the measured electrode potential is a realistic reflection of the potential that is applied across the enzyme/solution interface.

Relative Catalytic Rates as a Function of pH. The uniform decay of the enzyme activity allows subtraction of the currents of successive cycles to obtain background-corrected "difference" voltammograms, thereby affording a novel way to quantify the enzyme's catalytic performance over a continuous potential range. Difference voltammograms were calculated (ignoring the first cycle) from experiments carried out for 1:1 fumarate/succinate mixtures over a range of pH values, and examples obtained at pH 7.0, 7.5, and 8.0 are shown in Figure 4, in which they are compared with simulated voltammograms produced as described later. Three sets of ratios were determined: these were (A) succinate oxidation limiting current versus fumarate reduction peak current, i^{S}_{lim}/i^{F}_{peak}; (B) succinate oxidation limiting current versus fumarate reduction limiting current, i^{S}_{lim}/i^{F}_{lim}; and (C) fumarate reduction peak current versus fumarate reduction limiting current, i^{F}_{lim}/i^{F}_{peak}. Values of i^{F}_{lim} were frequently complicated by background slope which was more noticeable at high pH, and the ratio i^{F}_{lim}/i^{F}_{peak} was thus found to vary considerably from one experiment to another. Subtraction of different pairs of cycles, while producing different absolute currents, yielded the same ratios, i.e., the magnitude but not the shape is changed. The results are shown in Figure 5.

The Tunnel Diode Effect. As evident from Figure 4 and data shown in Figure 5, the fumarate reductase activity does not decrease to zero at very negative potentials, but instead drops sharply to a fairly constant level which is approximately 50% of the peak current. Values of i^{F}_{lim}/i^{F}_{peak} showed considerable scatter, but within reasonable error margins the ratio was independent of fumarate concentration and constant over the entire pH range. The non-zero limiting current at low potentials was also observed in experiments in which the potential was stepped between $E_{F/S}$ and regions corresponding to i^{S}_{lim}, i^{F}_{peak}, and i^{F}_{lim}, but was not observed, as expected, in experiments carried out in the presence of succinate alone. Close scrutiny of the background component of voltammograms showed no evidence for any sharp increase or decrease in capacitance in this region of potential.

It was suggested previously that the tunnel diode effect might arise if SDH has a greater affinity for fumarate when the FAD is oxidized.[12] However, experiments carried out with 1:1 succinate−fumarate concentrations ranging between 0.1 mM and 10 mM (where substrate levels are well in excess of concentrations required to saturate the enzyme[16,30]) showed the current ratios to be independent of the absolute concentration. We expect that if the effect is due to differences in fumarate binding affinities of FAD_{ox} and FAD_{red} forms, the decrease in current should be progressively quenched as the fumarate concentration is increased.[31] Experiments conducted with 10:1 fumarate−succinate ratios, although giving extremely unstable voltammetry, showed the same ratio i^{F}_{lim}/i^{F}_{peak} (within the

(29) The steady-state behavior may be due to having only a very small coverage of active enzyme, which should provide well-separated radial (rather than linear) diffusion trajectories for transport of substrate molecules to the sites of catalysis (ref 10).

(30) Kotlyar, A. B.; Vinogradov, A. D. *Biochim. Biophys. Acta* **1984**, *784*, 24−34

(31) This arises from consideration of simple Michaelis−Menten kinetics, since effects of binding equilibria become less significant as substrate concentrations become high enough to saturate the binding sites (i.e. [substrate] ≫ K_M).

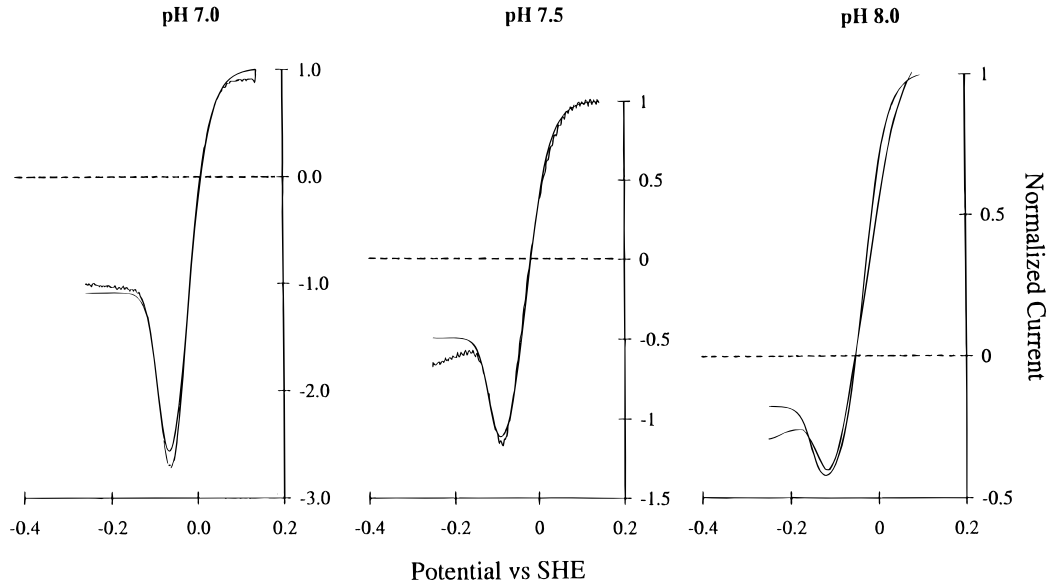

Figure 4. Difference voltammograms and simulation results obtained for the data presented in Figure 2, i.e. at pH values of 7.0, 7.5, and 8.0. The experimental results have been modified by background subtraction as described in the text and the parameters used in the model correspond to those presented in Figure 3.

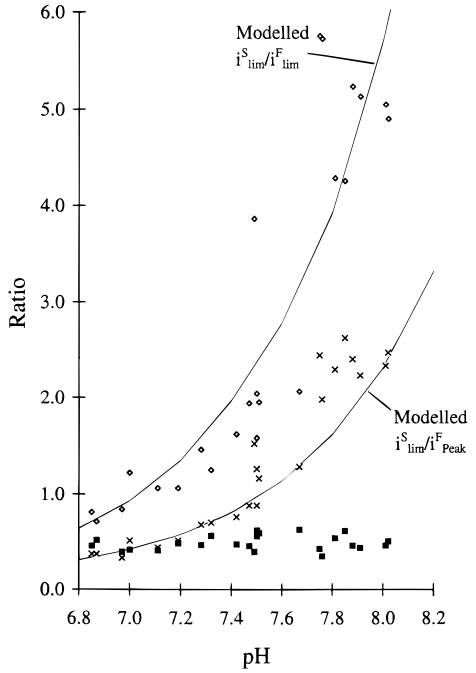

Figure 5. Experimentally determined current ratios, i^S_{lim}/i^F_{peak} (×), i^S_{lim}/i^F_{lim} (◇), and i^F_{lim}/i^F_{peak} (■) as a function of pH. Also shown (as lines) are the ratios i^S_{lim}/i^F_{peak} and i^S_{lim}/i^F_{lim} that are predicted by the model.

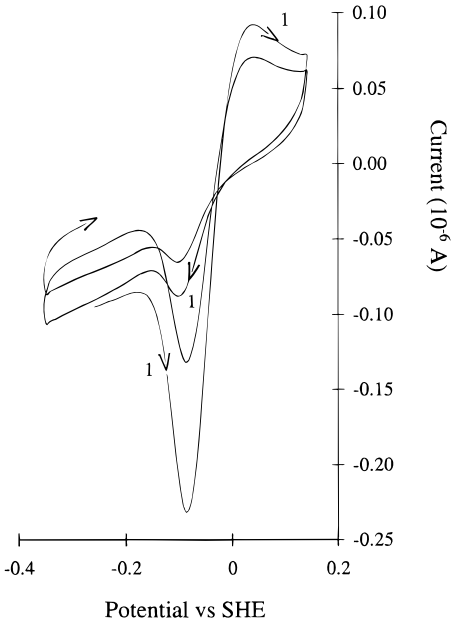

Figure 6. Cyclic voltammogram obtained in the presence of both fumarate and succinate (each at a concentration of 1.37 mM) and oxalacetate (concentration of 5.49 mM) at 10 mV s^{-1}, 500 rpm at pH 7.36. The peak shift and attenuation of the peak current on the reductive scan are clearly visible. The first cycle is labeled "1".

bounds set by the scatter of data) as observed for the 1:1 experiment. It was thus concluded that a redox-state dependent change in affinity for fumarate is not responsible for the tunnel-diode effect, an idea supported by values of K_D for fumarate or succinate reported in the literature which are small (tight binding) and vary only by approximately one order of magnitude with FAD oxidation state.[16,30]

Observations of Redox-Driven Binding and Release of Oxalacetate. More definitive information on the origin of the tunnel-diode effect was obtained from experiments in the presence of oxalacetate, a competitive inhibitor having a small preference (ca. 10-fold) for the FAD_{ox} form, but displaying slow binding kinetics.[18,30] From fluorescence quenching measurements, it is known that oxalacetate binds near to the FAD.[18] Figure 6 shows two successive voltammetric cycles obtained for a 1.5 mM:1.5 mM mixture of fumarate and succinate in the presence of 5 mM oxalacetate. At a scan rate of 10 mV s^{-1} there is a marked contrast between the high catalytic activity observed when scanning from negative to positive potential and the much lower activity observed when scanning in the reducing direction. The peak potentials no longer coincide, and E_{peak} for the reductive direction is noticeably shifted to a potential more negative than that observed in the absence of oxalacetate. Under the same conditions but at slower scan rates (2−5 mV s^{-1}), the appearance of oxidative and reductive scans become more similar, with i^F_{peak} magnitudes being comparable and E_{peak} coinciding for each scan direction.

These results are consistent with the behavior expected if the relative concentration of inhibitor is sufficient to inactivate most of the oxidized form but is low enough to allow release from

the reduced state. Accordingly, raising or lowering the oxalacetate concentration by 10-fold (the reported range of redox discrimination for oxalacetate binding) away from the above optimally sensitized conditions caused either total inhibition or zero inhibition, respectively. The discernible shift in E_{peak} also reflects this difference in binding affinities for oxidized vs reduced enzyme,[30] which should give rise to a maximum shift of ca. 61/*n* mV at 38 °C, where *n* is the number of electrons (2) transferred in the FAD reaction. Qualitatively, the rather slow kinetics of inhibitor binding are also readily observable. For succinate oxidation as viewed in the direction of increasing potential, the increasing current only just outweighs the rate of inactivation by inhibitor binding, and a decay of the limiting current is observed at high potential. On the reverse scan, the fumarate reduction peak is attenuated, but thereafter the enzyme becomes reactivated as the inhibitor is released. As the scan rate is decreased, the two catalytic profiles become more similar in appearance, reflecting equilibration of the system during scanning. Together with the previously established oxalacetate−FAD interaction, these results provide compelling evidence that the tunnel diode effect is linked to the redox status of the FAD group, a hypothesis further supported by the data analysis described below.

4. Interpretation of the Voltammetry via Use of a Model

General Description of the Model. For catalysis of a solution redox reaction by a surface-bound redox couple, the extent to which catalysis is favored in one direction over the other depends, in the first instance, on how the thermodynamic properties of the catalyst are biased with respect to the reduction potential of the solution couple. For succinate dehydrogenase and other multi-centered enzymes, this "tuning" reflects complicated, *collective* effects of the ensemble of redox centers—effects that are not easily visualized experimentally or manifested in separate observations of individual centers. As in other electrocatalytic studies of enzymes, determinations of K_M and k_{cat} in either direction are hindered by instability and by the fact that the coverage of active enzyme is unknown. Therefore, instead of attempting to measure absolute rates, we have focused on *relative* rates of substrate interconversion and used quantities that could be measured precisely and continuously across a wide potential range. The enzyme's catalytic action can then be expressed instead in terms of a *thermodynamic* cycle which comprises a series of reversible binding (K_D) and catalytic ($k_{cat}^{forward}/k_{cat}^{back}$) equilibria controlling transfer of the two electrons required for substrate transformation. The model is shown in Scheme 1.

Scheme 1

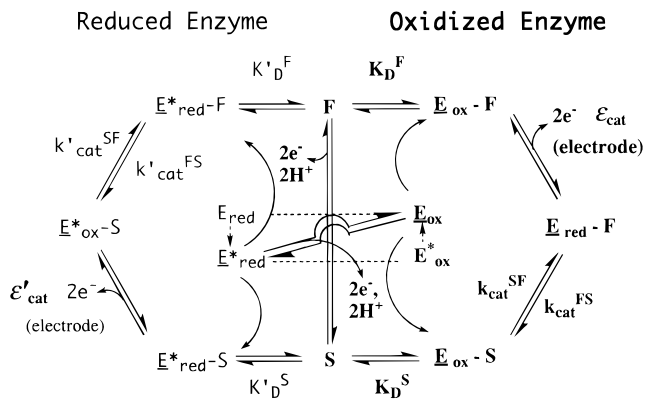

The right- and left-hand cycles of Scheme 1 are linked by the substrate reaction, i.e. the reversible interconversion of fumarate and succinate (the equilibrium potential of which is $E_{F/S}$) but they differ in the choice of active-site conformations participating in the formation of the enzyme−substrate complexes. The two conformations are denoted as $\underline{E}_{ox}/E_{red}$ and $E^*_{ox}/\underline{E}^*_{red}$, an asterisk being used to identify the less-active form of the enzyme, with underlined species being the most stable. Conversion from $\underline{E}_{ox}$ to $\underline{E}^*_{red}$ at low potential is thus responsible for the tunnel-diode effect. This interconversion takes the form of a square scheme, in which E_{red} converts spontaneously to $\underline{E}^*_{red}$ and E^*_{ox} reverts back to $\underline{E}_{ox}$. Since the lifetimes of FAD oxidation states on the catalytic cycles are very short, conformational interconversions depend upon the steady-state level that can be maintained by the applied potential. Each cycle also contains reference to a parameter, E_{cat}, which is the "effective" half-wave potential for electron exchange between the electrode and the catalytic centers of the enzyme. This is of intrinsic significance, since the deviation of E_{cat} from $E_{F/S}$ quantifies the degree to which various redox centers in the enzyme, acting collectively, provide the bias to favor reaction in one direction relative to the other.

Mathematical Formulation. We first consider the *underlying* characteristics of the enzyme, i.e. the behavior expected in the absence of the tunnel diode effect, and thus restrict ourselves to considering only the right-hand cycle. Since the sum of the free energy changes for steps in each half of the cycle must equal zero, we write, in the case of equal activities of succinate and fumarate:

$$RT \ln K_D^{\,F} - 2FE_{cat} - RT \ln\left(\frac{k_{cat}^{FS}}{k_{cat}^{SF}}\right) - RT \ln K_D^{\,S} + 2FE_{F/S} = 0 \quad (3)$$

and therefore

$$E_{cat} - E_{FS} = \frac{RT}{2F} \ln\left(\frac{K_D^F k_{cat}^{SF}}{K_D^S k_{cat}^{FS}}\right) \quad (4)$$

where the bracketed quotient is the ratio of specificity constants (second-order rate constants) if $K_D \approx K_M$.[32] Equation 4 thus defines *quantitatively* the enzyme's bias (to perform in one particular redox direction) in terms of the difference between E_{cat} and E_{FS}.

We are now in a position to compute the shape and position of the catalytic wave. Our approach exploits the comparative simplicity of the system, i.e. the reversibility of electron transfer and bidirectionality of catalysis, and the steady-state characteristics.[33] We consider the result expected if interconversion of fumarate and succinate (at equal activities) were to be electrochemically reversible at a bare (non-catalytic) electrode or at an electrode modified with a catalyst that displays no directional bias. For *reversible* (Nernstian) electron exchange, the wave shape under steady-state conditions is described by eq 5.[34]

$$\frac{i_S}{i_F} = \exp\left\{\frac{n_{cat}F}{RT}(E - E_{cat})\right\} \quad (5)$$

(32) See for example: Fersht, A. In *Enzyme Structure and Mechanism*, 2nd ed.; W. H. Freeman: New York, 1985.

(33) The steady-state behavior observed is in contrast to results described in recent papers for catalysts adsorbed at monolayer coverage on stationary electrodes (Xie, Y.; Anson, F. C. *J. Electroanal. Chem.* **1995**, *384*, 145−153 and references therein).

(34) See for example: Bard, A. J.; Faulkner, L. R. *Electrochemical Methods*; J. Wiley: New York, 1980.

The terms i_S and i_F are the currents due to succinate oxidation and fumarate reduction, respectively, at potential E; E_{cat} is the relevant half-wave potential and n_{cat} is the number of electrons transferred across the electrochemical transition state, which could in this case be either one or two (although the total number of electrons transferred per chemical conversion, eq 1, must equal two). The bias of the enzyme to act in one particular direction expected from eq 4 is then introduced by transposing the wave along the E and i axes to fulfill the condition that the potential of zero current must be $E_{F/S}$.

Further refinement required incorporation of the tunnel-diode effect into the model. This was achieved by including a second Nernstian couple, associated with a reduction potential, E_{switch}, which interconverts the active form of the enzyme $\underline{E}_{ox}$ (right-hand side of Scheme 1) and the less-active form $\underline{E}^*_{red}$ (left-hand side),

$$\phi = \left\{1 + \exp\left\{\frac{nF}{RT}(E_{switch} - E)\right\}\right\} \qquad (6)$$

where ϕ is the fraction of less-active form, i.e. $\underline{E}^*_{red}/(\underline{E}_{ox} + \underline{E}^*_{red})$ and E is the applied electrode potential.

Modeling Parameters and Results. Simulation of the voltammetry requires input of the parameters $E_{F/S}$, E_{cat}, E_{switch}, n_{cat}, n, experimental temperature, and a value for the activity of $\underline{E}^*_{red}$ relative to $\underline{E}_{ox}$. It is expected that the three potential variables may show pH dependence: $E_{F/S}$ is the isosbestic potential, the characteristics of which are known accurately from the experimental data (Figure 3) and E_{switch} is the potential of the switch (associated with the FAD and anticipated to be pH dependent due to the transfer of n electrons and m protons). We are not in a position at present to suggest the definition of anything other than an empirical pH dependence for E_{cat}. In order to obtain values for n_{cat}, E_{switch}, n and m, E_{cat}, and the relative activities, the simulation parameters were adjusted until the fit between predicted and experimental results was optimized (according to the criteria of the peak potential and the three current ratios shown in Figure 5). Typical calculated difference voltammograms are overlaid on the experimental results shown in Figure 4. The comparison between calculated and observed current ratios is given in Figure 5 and calculated peak potentials are included in Figure 3. As can be seen, the model yields a good fit to the data, particularly at lower pH where the experimental scatter is smaller.

The following information can now be derived:

(i) The underlying catalytic wave shape in the reversible region for succinate/fumarate interconversion is that of a one-electron process (i.e. $n_{cat} = 1$). No satisfactory fit to the data could be obtained using $n_{cat} = 2$. This is consistent with electron transfers from the electrode to the enzyme occurring in one-electron steps.

(ii) E_{cat} has a small pH dependence (ca. 10 mV per decade) as given in Figure 3.

(iii) The ratio of specificity constants, defined in eq 4 as a function of the difference between E_{cat} and $E_{F/S}$, shows a strong pH dependence. The calculated ratios are presented in Figure 7.

(iv) By using $n = 2$ and $m = 2$, excellent agreement is obtained between the experimentally measured and theoretically calculated values of E_{peak} over the whole pH range. No reasonable fit could be obtained using n or m values of 1. Both the pH dependence and the optimized potential values for E_{switch} (-90 mV at pH 7.0, -120 mV at pH 7.5, and given in Figure 3) are similar to those previously reported (E_{12}) for the FAD/$FADH_2$ couple.[17,18]

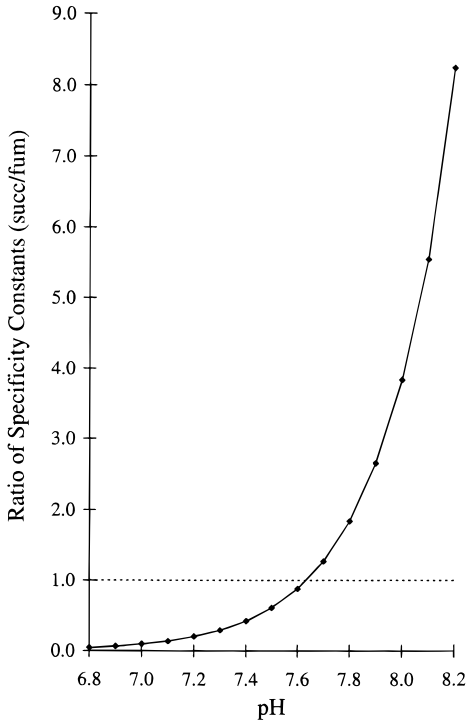

Figure 7. Calculated ratio of specificity constants (succinate/fumarate) as a function of pH, as calculated from eq 4.

(v) The less active, low-potential form has 30−40% of the activity of the fully active form over the pH range studied.

5. Discussion

The comparison between the potential imposed by the substrate ($E_{F/S}$) and the catalytic potential (E_{cat}) reveals that in the thermodynamically reversible region of the fumarate/succinate redox couple, succinate dehydrogenase is energetically biased to catalyze in the direction of fumarate reduction at pH values below 7.64. This is clearly seen in Figure 3, from the crossover point between $E_{F/S}$ and E_{cat}, and from Figure 7, which shows the calculated ratios of specificity (second-order rate) constants for succinate oxidation compared to fumarate reduction, as a function of pH. The pH dependence of these activities is consistent with the results obtained by Vik and Hatefi[35] but is in disagreement with the more recent results of Vinogradov and co-workers, who found that fumarate reductase and succinate dehydrogenase activities of detergent-solubilized Complex II each *increased* with *increasing* pH.[36] Previous literature reports based upon studies that use $Fe(CN)_6^{3-}$ as electron acceptor, or *low-potential* dyes such as benzyl viologen as electron donors, have invariably described the activity of SDH to be higher in the direction of succinate oxidation.[16] However, considered alone, the FAD group with a reported reduction potential of -79 mV (at pH 7) is much better suited to reduce fumarate. The conditions of temperature (38 °C), the range of pH, and an electrochemical potential in the region of the fumarate/succinate couple are believed to be those prevailing inside the mitochondrial matrix under physiological conditions.[37] Thus SDH is predicted to function *reversibly* under physiological conditions.

(35) Vik, S. B.; Hatefi, Y. *Proc. Natl. Acad. Sci. U.S.A.* **1981**, *78*, 6749−6753.

(36) Grivennikova, V. G.; Gavrikova, E. V.; Timoshin, A. A.; Vinogradov, A. D. *Biochim. Biophys. Acta* **1993**, *1140*, 282−292.

(37) Assuming an external (cytoplasmic) pH of 7.2 and a value of ΔpH $\leq$0.5 across the inner mitochondrial membrane (Ferguson, S. J.; Sorgato, M. C. *Annu. Rev. Biochem.* **1982**, *51*, 185−217), the pH of the matrix is expected to be $\leq$7.7.

The relatively positive value of E_{cat} (−25 mV at pH 7.0) indicates the influence on the catalytic energetics of centers other than the FAD, thus raising the fundamental question as to how individual characteristics combine to determine the operative potential of a complex enzyme. The one-electron nature of the catalytic wave shape in the thermodynamically reversible region and the small pH dependence of E_{cat} (ca. 10 mV per pH unit) suggest that one or more of the Fe−S clusters (in addition to mediating electrons between the FAD and the electrode) are key factors in determining the preferred direction of catalysis. From the published potentiometric results[16] the likely candidates are Center 1 (0 mV) and Center 3 (60 mV), and the resulting effect as reflected in E_{cat} is a complex combination of the individual thermodynamics and kinetic capabilities of the contributing redox sites. These considerations will also apply to other multi-centered electron-transport enzymes, for which the catalytic energetics may not be so readily measured.

From the data presented, we conclude that reduction of the FAD is responsible for the tunnel-diode effect. First, a $2e^-/2H^+$ dependence is necessary to obtain a fit, and the cooperative two-electron nature of the group responsible is also obvious from the narrow width of the peak. Second, oxalacetate, a competitive inhibitor binding close to the FAD, has a marked effect on the amplitude and position of the peak. The evidence that this effect does not arise from changes in fumarate binding equilibria leads us to consider other possible ways in which reduction of the FAD could alter the rate of catalysis. Most obviously, a conformational change may occur upon formation of $FADH_2$; indeed, conformational changes have been noted for other flavoproteins—flavodoxin and benzoate hydroxylase.[38] Such a switch might influence the rate in several ways, for example by increasing intramolecular electron- or proton-transfer distances, decreasing the rate of succinate release, or even decreasing rates of substrate binding and release *equally* (thus not affecting K_D). While the origin of the effect remains unclear, the important point to note is that an effect amounting to a comparatively small (but abrupt) alteration in catalytic rate as different centers of the enzyme are redox-switched can be so readily detected as an *irregularity*, in a single experiment. The advantage of being able to measure an enzyme's electron-transport performance across a continuous function of potential is clearly displayed. Significantly, no irregularity is observed in the region positive of E_{peak}, thus showing that oxidation and reduction of Fe−S Centers 1 and 3 does not induce changes in the electron-transport rate. Neither is any irregularity observed in the region of potential reported for Center 2 (−260 mV).[16,19]

The physiological significance of these results is unclear, a major problem being that the enzyme under study is not the intact membrane-bound complex, but the soluble membrane extrinsic domain. However, the fact that SDH acts bi-directionally in this experiment renders it very likely that a similar situation will hold for Complex II. The tunnel-diode effect could provide a means for fine control of the TCA cycle as a function of the status of the quinone pool, most obviously under conditions of oxygen deficit in which the quinone pool potential may become very low (State 4 respiration).[39]

The broad conclusions of this work are that enzymes which have strong electronic coupling with the electrode (electro-activity) and which are capable of displaying high rates of substrate turnover can be studied to reveal characteristics that are not apparent from conventional studies. Most obviously an intimate link between driving force and rates is defined, thereby allowing the performance of an electron-transport enzyme to be measured in a similar fashion to components of electronic circuitry. The degree to which an enzyme is biased to catalyze more effectively in one direction over the other can be quantified, and the ability to scan across a continuous potential range enables the detection of small changes in electron-transport activity occurring as sites switch between redox states. Oxidation-state-dependent interactions with inhibitor/regulator molecules in solution are also easily observed. Extensions of this methodology to other enzymes of electron-transport chains are currently under way.

Acknowledgment. This work was funded by The Wellcome Trust (Grant No. 042109), the UK EPSRC, and the U.S. National Institutes of Health (USPHS Program HL-16251). J.H. and F.A.A. thank Wadworth 6X administered by the Kings Arms for valuable assistance.

JA9534361

(38) Gatti, D. L.; Palfey, B. A.; Myoung, S. L.; Entsch, B.; Massey, V.; Ballou, D. P.; Ludwig, M. L. *Science*, **1994**, *266*, 110−114. Watt, W.; Tulinsky, A.; Swenson, R. P.; Watenpaugh, K. D. *J. Mol. Biol.* **1991**, *218*, 195−208.

(39) Kröger, A. *Methods Enzymol.* **1978**, *53*, 579−591.